

Short Communication

## Effect of UV Illumination on the Corrosion Behavior of Under a Thin NaCl Electrolyte Layer

Cunsheng Zhao<sup>1,\*</sup>, Kunjie Dai<sup>2</sup>, Puhua Li<sup>2</sup>, Zhanming Cheng<sup>2</sup>, Kui Xiao<sup>2,\*</sup>

<sup>1</sup> College of Naval Architecture and Ocean Engineering, Naval University of Engineering, Wuhan 430033, China

<sup>2</sup> Corrosion and Protection Center, Institute for Advanced Materials and Technology, University of Science and Technology Beijing, Beijing 100083, China

\*E-mail: [zhaocunsheng@hotmail.com](mailto:zhaocunsheng@hotmail.com), [xiaokui@ustb.edu.cn](mailto:xiaokui@ustb.edu.cn)

Received: 18 July 2022 / Accepted: 10 October 2022 / Published: 20 October 2022

---

The corrosion behavior of 304 stainless steel (SS) under a liquid NaCl thin film was investigated by analyzing the corrosion morphologies, polarization curves, Mott-Schottky (M-S) measurements and transient photocurrent experiments. The results revealed that ultraviolet (UV) illumination promoted pitting nucleation and growth. An extremely rapid oxygen supply caused shallow pitting areas on the UV-irradiated specimen surface. Light-responsive passive films appeared on the surface of the pre-passivated stainless steel. In addition, the corrosion process of 304 SS under thin NaCl electrolyte layer with UV irradiation was influenced by the photovoltaic effect of semiconductor corrosion products.

---

**Keywords:** 304 Stainless steel; pitting corrosion; thin NaCl electrolyte layer; UV illumination

### 1. INTRODUCTION

Due to its superior mechanical properties and corrosion resistance, 304 SS is widely used in outdoor engineering and construction [1, 2]. However, in practical situations, it is particularly susceptible to corrosion when in contact with the environment, especially leading to the formation of a thin liquid film containing Cl<sup>-</sup> due to condensation in a marine atmosphere. Cl<sup>-</sup> damage typically manifests in the rupturing of the passivation film, leading to severe pitting and impacting the rust layer composition [3, 4].

Over the past few decades, several studies have examined the influence of environmental factors on atmospheric metal corrosion, primarily focusing on temperature [5-7], relative humidity [8-10], salt particles in the air [11-14], and stainless steel composition [15]. Ultraviolet (UV) light has recently started to attract considerable research attention as a possible influencing factor. However, the effects of UV light on the corrosion mechanism of stainless steel have not been fully understood and were currently

discussed in the solution system [16-21]. Macdonald found that the pitting resistance of stainless steel varied significantly at different power densities [16]. The inhibitory effect of light on the corrosion of stainless steel was investigated, revealing that UV illumination inhibited the proliferation of pits in 304 SS and 316SS in solutions containing chlorine [17-18]. Luo [19] indicated that UV light irradiation improved the stability of passive films in acid solutions, possibly affecting the film composition. Breslin [20] revealed that UV light enhanced the passive film produced on 316 SS in neutral solutions. Fujimoto discovered that UV irradiation mitigated pitting corrosion [21]. The corrosion behavior of stainless steel under a thin liquid film is substantially different from that in solutions. Contrary to the solution system, UV light accelerated the corrosion of carbon steel [22, 23] and weathering steel [24, 25] in an atmospheric environment. These studies attributed the accelerated corrosion of metals by UV irradiation to the photoelectric effect of semi-conductive corrosion products. However, using UV irradiation, Guo [26] conducted an accelerated corrosion test of wet-dry cycles in a simulated salt lake environment. The results revealed that light promoted the formation of a dense  $\text{Cr}_2\text{O}_3$  film, while UV irradiation slowed the corrosion of 316 SS with extended corrosion time.

Minimal studies are available regarding the effect of UV light on the corrosion behavior of stainless steel under a thin electrolyte layer containing chlorine. Moreover, the influence of UV illumination on the corrosion of stainless steel are still controversial. This paper designed a method to adjust the thickness of a thin electrolyte layer in a NaCl solution to examine the impact of UV on the corrosion behavior and mechanism of 304 SS.

## 2. EXPERIMENTAL DESIGN

### 2.1. Experimental material and design

A 304 SS (hot rolling sheet) with a chemical composition (wt.%) of Cr 18.0, Ni 9.0, Mn 2.0, Si 1.0, C 0.07, P 0.035, S 0.030, balanced by Fe was used. Plate specimens of 10 mm × 10 mm × 4 mm were cut and sealed with epoxy, while a 1 cm<sup>2</sup> surface area served as the working electrode for the electrochemical tests. Before the tests, the surface was ground with 800 grit SiC paper, degreased in alcohol, cleaned with distilled water, and dried in warm air. The treated working electrode was centered in a Teflon cylinder which was solidly anchored in the cell (Figure 1).

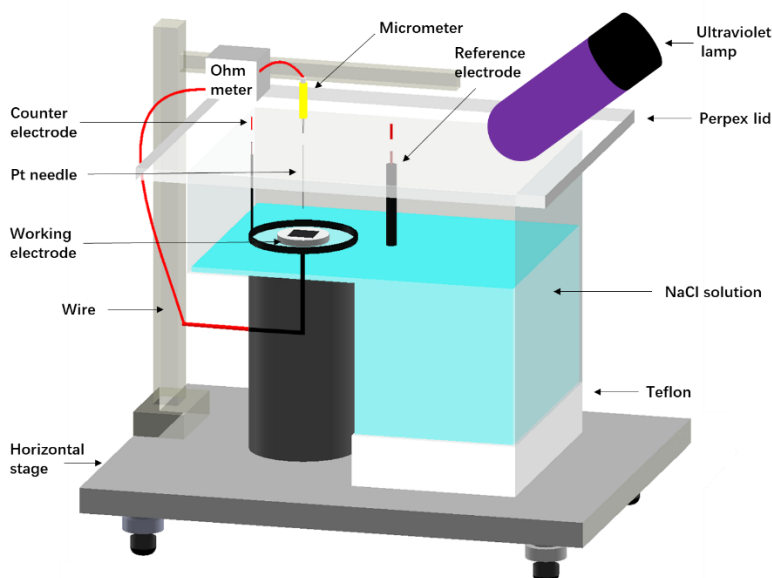


**Figure 1.** A schematic diagram of the equipment to adjust the thin electrolyte layer thickness.

A controllable liquid film electrochemical device was placed horizontally on a platform that could be adjusted using a gradienter. The liquid level was parallel to the electrode surface after adjustment. In this experiment, a micrometer with a platinum tip, a battery, and an ohmmeter was used to measure the thickness of the electrolyte layer. A sudden change was evident in the current when the Pt needle came into contact with the electrolyte layer, followed by an additional rapid change when the Pt needle touched the metal surface. The distance the platinum needle moved between the two current changes represented the thickness of the NaCl electrolyte layer. The electrolyte film thickness was controlled at 200  $\mu\text{m}$  using a micrometer, as shown in Figure 1, the specific operational method of which was described elsewhere [27]. The experimental light source was a Spectro-line EB-160C UV lamp with a central wavelength of 312 nm and a light intensity of 400  $\mu\text{W}/\text{cm}^2$ . A quartz glass sheet was added to cover the cell to prevent thermal impact and electrolyte evaporation.

## 2.2. Electrochemical measurements

The anodic polarization curves were measured using a PARSTAT 2273 workstation. A three-electrode system was used to obtain the anodic polarization curve, as shown in Figure 1. The working electrode consisted of 304 SS, while the counter electrode was a circle-type Pt wire. Furthermore, the reference electrode used in this paper was a saturated calomel electrode (SCE). The 0.5% NaCl experimental solution was prepared using analytically pure NaCl and deionized water, while the experiments were performed at room temperature.

A scanning rate of 0.33 mV/s was used during the polarization curve test, and the experiment was terminated when the anode current density increased to about 120  $\mu\text{A}$ . Moreover, the corresponding voltage value was marked as breakdown voltage  $E_b$  when the anode current density suddenly increased. The polarization curve test was followed by potentiostatic polarization at 150 mV<sub>SCE</sub> for 30 min while

recording the anode current density change with time. After anodization for 30 min at  $-50 \text{ mV}_{\text{SCE}}$ , these experiments were repeated to investigate the sensitivity of the passive film to UV light. In addition, Mott-Schottky (M-S) tests were conducted on the films at a frequency of 1000 Hz during a 20 mV/Step in a potential range of -0.3 V to 0.2 V (SCE). The electronic properties of the passive film were discussed after performing phototransient current tests on the thin NaCl electrolyte layer to further explore the effect of UV light on 304 SS film.

### 2.3. Corrosion morphology observation

The corrosion morphology of the samples after the polarization tests were observed using a stereomicroscope. In addition, scanning electron microscopy (SEM, XL30FEG) was used to obtain the surface micro-morphology of 304 SS in different conditions.

## 3. RESULTS AND DISCUSSION

### 3.1. Electrochemical measurements

The polarization curves of 304 SS under a 0.5% NaCl liquid film, with or without UV exposure,

are shown in

**Figure 2.** Regardless of anodization, the pitting potential of the sample exposed to UV light was distinctly lower than without UV light exposure. As shown in Table 1, pitting under the thin electrolyte layer was more likely to occur after UV illumination and was more pronounced when the passive film thinner was not pre-passivated.

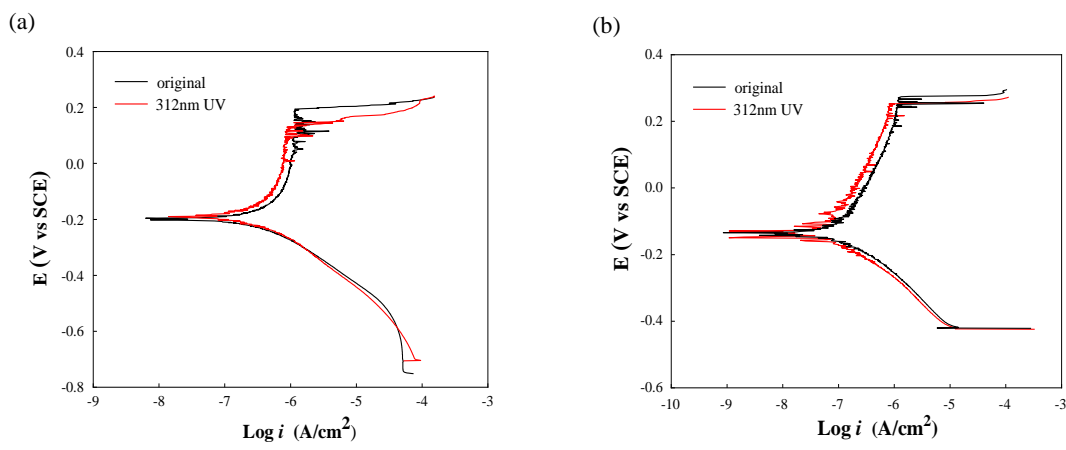


**Figure 2.** The polarization curve of 304 SS under a thin electrolyte layer with and without UV exposure. (a) The substrate sample and (b) The anodized sample.

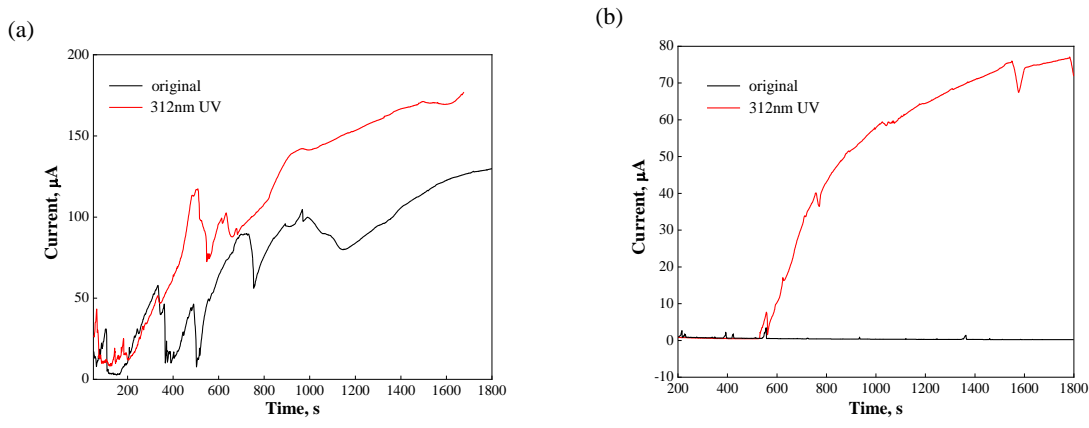


**Figure 3.** The anode current time curve of 304 SS at +150 mV<sub>SCE</sub> potentiostatic polarization with and without UV irradiation. (a) The substrate sample and (b) The anodized sample.

**Table 1.** The effect of UV on the pitting potential  $E_b$  and potential difference  $\Delta E_b$  of 304 SS under a thin electrolyte layer.

Condition	$E_{b \text{ light}}$ (mV <sub>SCE</sub> )	$E_{b \text{ dark}}$ (mV <sub>SCE</sub> )	$\Delta E_b$ (mV <sub>SCE</sub> )
Substrate sample	131	197	66
Anodized sample	253	277	24

The relationship curve between the anode current and time during potentiostatic polarization is shown in The polarization curve of 304 SS under a thin electrolyte layer with and without UV exposure. (a) The substrate sample and (b) The anodized sample.

**Figure 3.** In the absence of anodization, the anodic current increased with time, both with and without light exposure. Some fluctuations were evident within 600 s due to the self-healing ability of the stainless steel passive film, exceeding 100  $\mu\text{A}$  after 1800 s. In addition, the anode current density was accelerated by UV light, indicating more rapid development of pitting corrosion with more severe damage. The passive film produced via anodization was thicker and less prone to deterioration. Consequently, 304 SS showed excellent self-healing ability in the absence of UV light [28]. Although the anodic current was small and fluctuated no more than 5  $\mu\text{A}$ , it gradually moved out from the control of the UV light and increased significantly with time after about 550 s.

### 3.2. Analysis of corrosion morphology

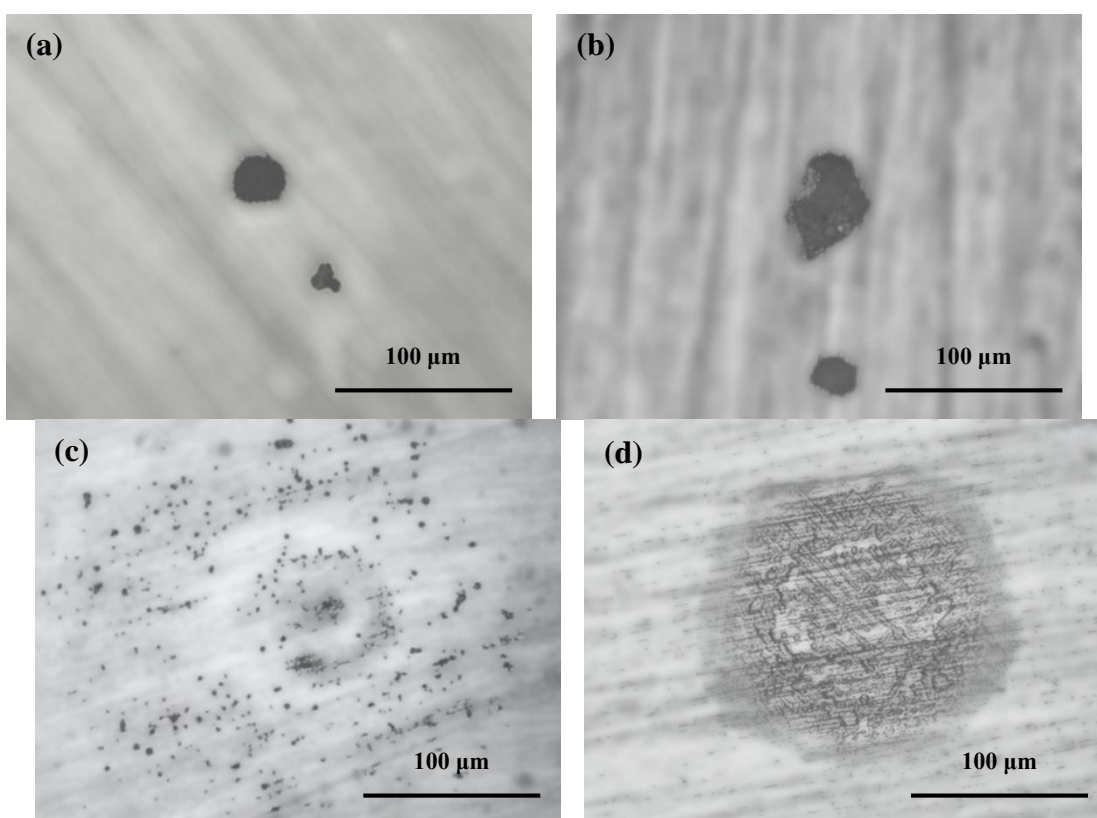


Figure 4 shows the pitting morphology of 304 SS under a NaCl thin film with and without UV illumination. Compared with the unexposed sample, UV irradiation had a pronounced influence on the pitting morphology of 304 SS surface after polarization. Although the overall pitting was minimal without illumination, the individual pits were substantially larger

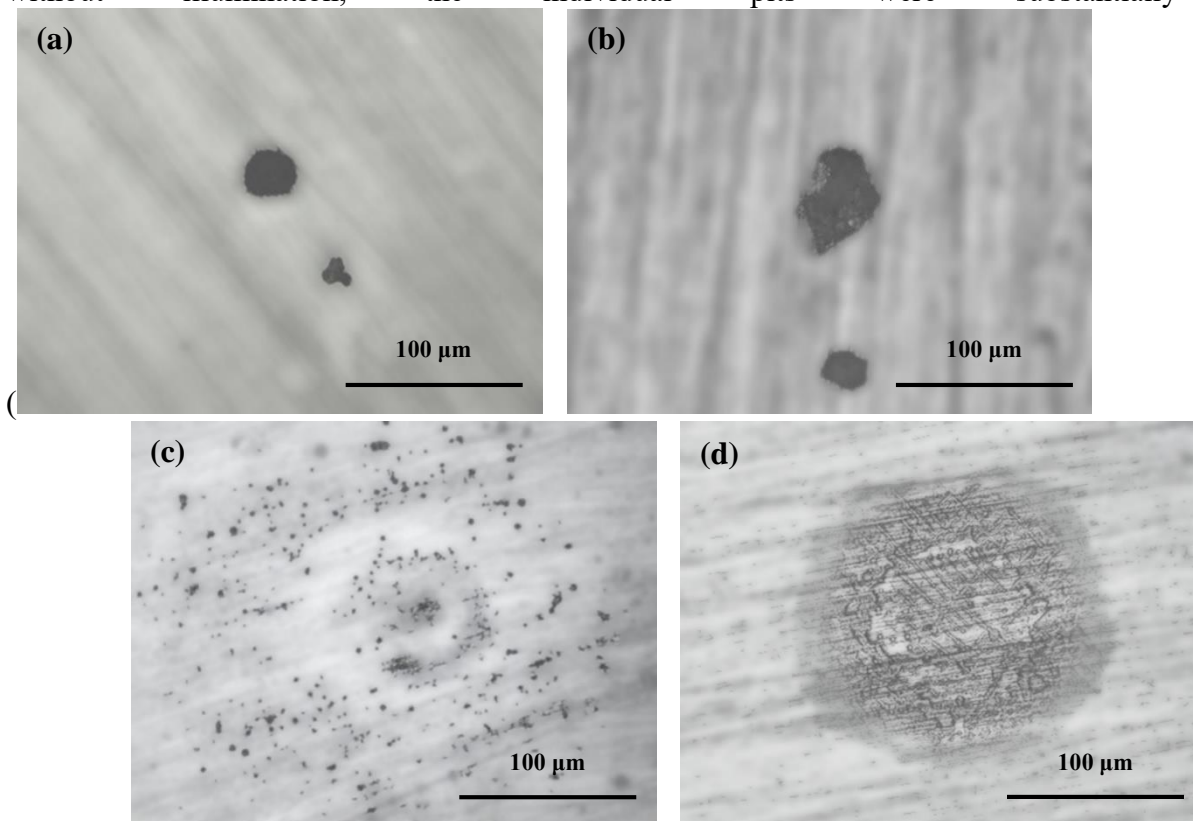
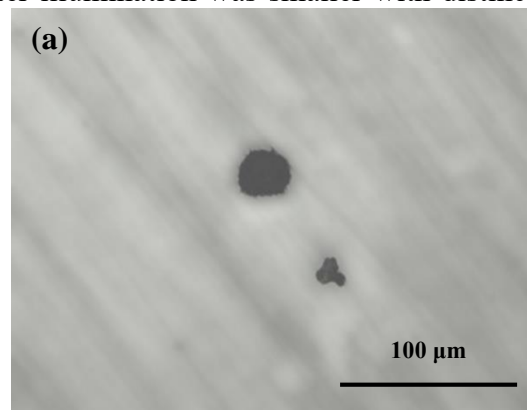
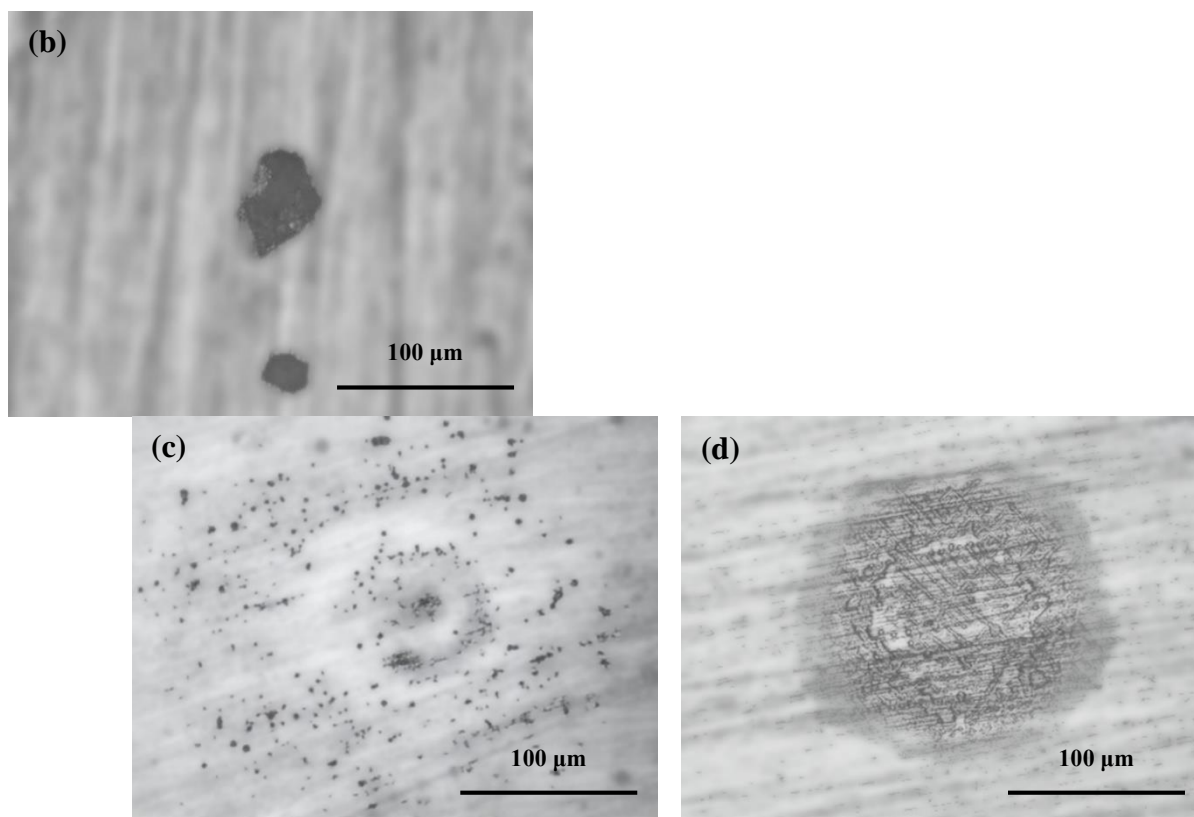


Figure 4a). However, much of the pitting formed after illumination was smaller with distinct

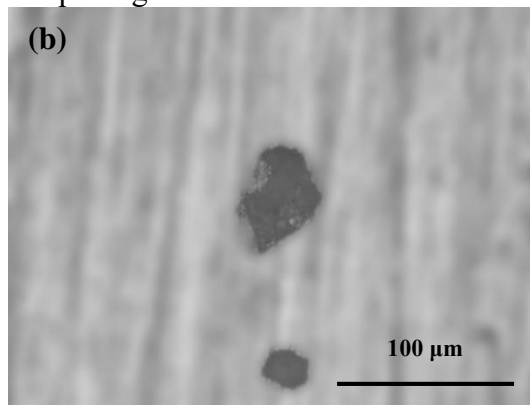
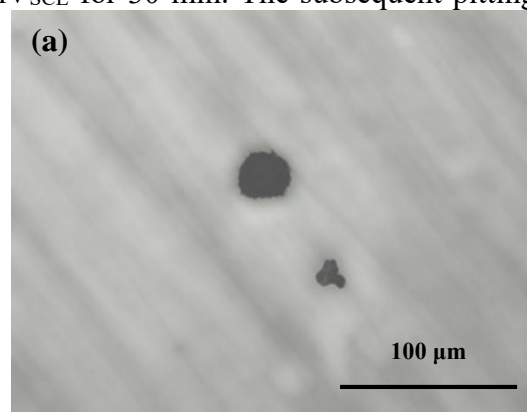
circular distribution around the central pit (





**Figure 4c)**, which could be attributed to the horizontal diffusion of metal cations under the thin liquid film [29]. The two samples were polarized at +150 mV<sub>SCE</sub> for 30 min. The subsequent pitting

morphologies are shown in



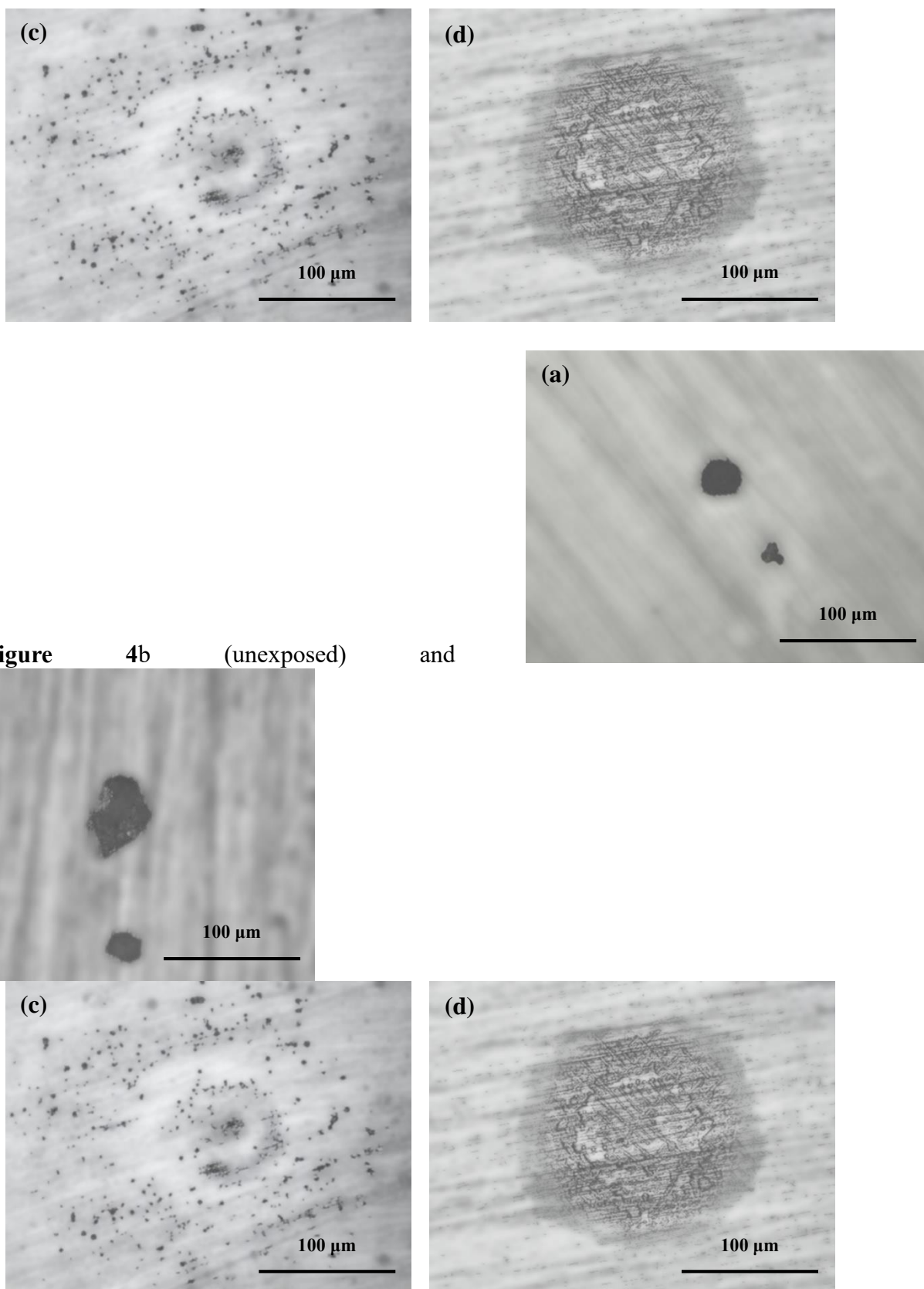


**Figure 4d (exposed).** After potentiostatic polarization, the pits proliferated significantly in the dark, but no new corrosion pit nucleation occurred. Interestingly, the formation of a large, shallow pitting zone with small, discrete pits was evident after UV illumination.

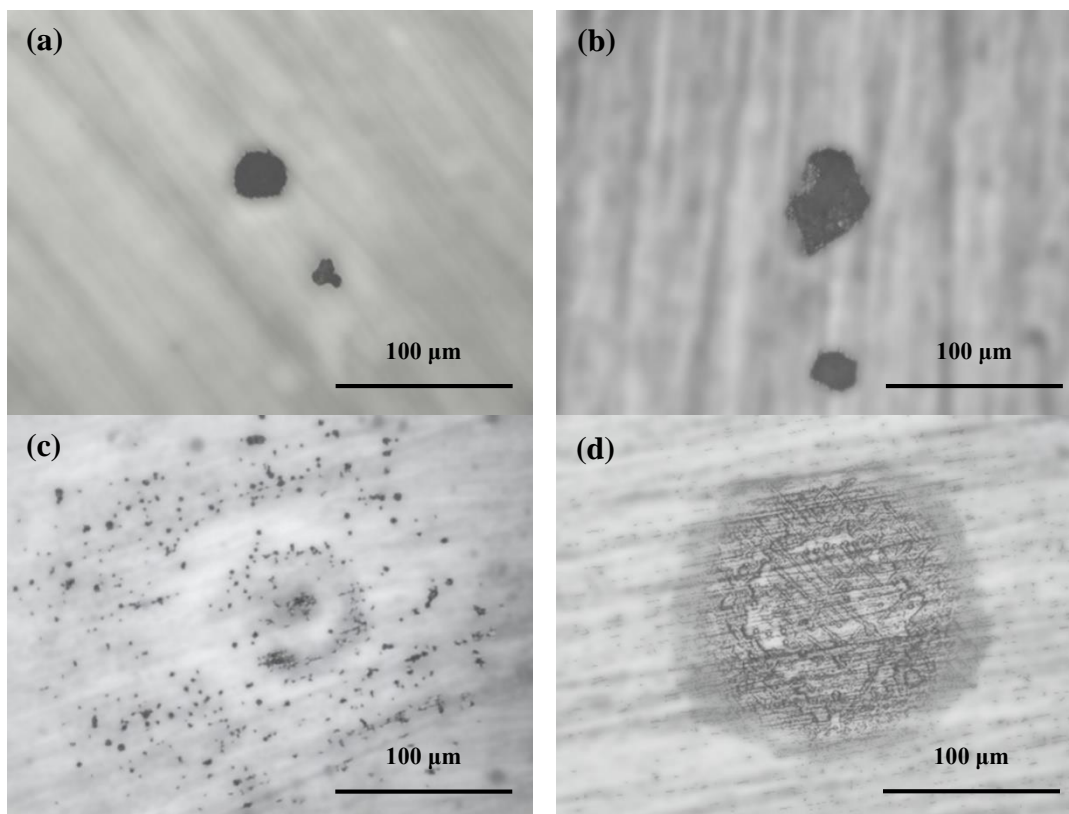


**Figure 4.** The pitting morphology of 304 SS under a thin NaCl electrolyte layer with and without UV irradiation. (a) Potentiodynamic polarization, (b) Potentiodynamic polarization + 30 min potentiostatic polarization, (c) UV irradiation + potentiodynamic polarization and (d) UV irradiation + potentiodynamic polarization + 30 min potentiostatic polarization.

During the early corrosion stage,  $\beta$ -FeOOH and  $\gamma$ -FeOOH were preferentially generated in the NaCl environment. While under UV illumination, the unstable  $\beta$ -FeOOH and  $\gamma$ -FeOOH were spontaneously converted to stable  $\alpha$ -FeOOH [23] and were cathodically reduced with metal ions using the following equation:



The cathodic reaction promoted  $Fe_3O_4$  formation in the UV samples. The  $Fe_3O_4$  with good conductivity [25] obtained under light might be the reason for the formation of pitting areas.

### 3.3. M-S measurements

The M-S plots of the passive film under the thin NaCl electrolyte layer with and without UV illumination are shown in Figure 5. The passive film of 304 SS was obtained by applying  $-50 \text{ mV}_{SCE}$  potential after 30 min of polarization. The two nonlinear M-S curves in Figure 5 may be caused by surface states or the uneven distribution of donors [30]. Positive slopes were obtained in the potential test region, confirming that the passive film was n-type semi-conductive film in two cases. The M-S

equation of the n-type semiconductors is as follows [31]:

$$\frac{1}{C^2} = \frac{2}{\epsilon\epsilon_0 e N_D A^2} (E - E_{fb} - KT / e) \tag{2}$$

where  $\epsilon$  is the dielectric constant of the passive film (set as 15.6, refer to [32]),  $e$  is the electron charge ( $1.602 \times 10^{-19}$  C),  $\epsilon_0$  is the dielectric constant of the free space ( $8.85 \times 10^{-14}$  F/cm),  $K$  is the Boltzmann constant ( $1.38 \times 10^{-23}$  J/K),  $T$  is the absolute temperature, and  $N_D$  is the donor density of the passive film.  $E$  and  $E_{fb}$  are the applied electrode and flat band potentials, respectively. Linear fitting obtained the donor density and flat band potential values, as shown in Table 2.

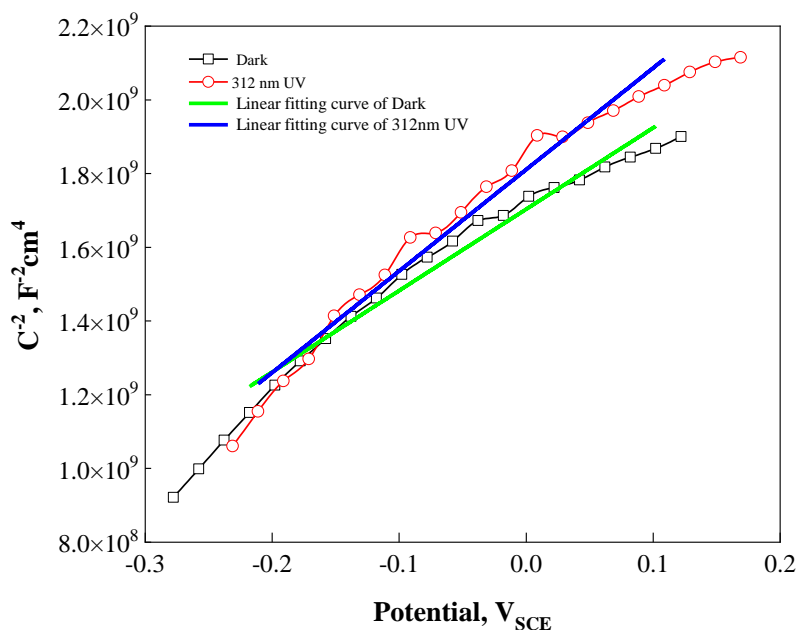


**Figure 5.** The M-S curve of 304 SS under a thin NaCl electrolyte layer with and without UV irradiation after anodization.

**Table 2.** The effect of UV irradiation on semiconductor properties of 304 SS passive film.

Condition	M-S curve slope	$N_D$ ( $10^{21}$ at $\text{cm}^{-3}$ )	$E_{fb}$ ( $V_{SCE}$ )
Without UV	$2.21 \times 10^9$	4.09	-0.79
With UV	$2.75 \times 10^9$	3.29	-0.67

Compared with the unexposed passive film, the light-exposed film displayed higher flat band potential and lower donor density. Several studies [333435] indicated that the  $N_D$  value was negatively correlated with passive film resistance. The passive film is more susceptible to pitting at a higher  $N_D$  value. However, this paper has shown that UV light may promote 304 SS pitting nucleation.

### 3.4. Analysis of the corrosion behavior of the passive film

To examine whether spontaneously formed passivation film and that generated via anodic polarization displayed a significant photoresponse in sufficient oxygen conditions, the photoresponse

currents were measured at their film forming potential, as shown in Figure 6.

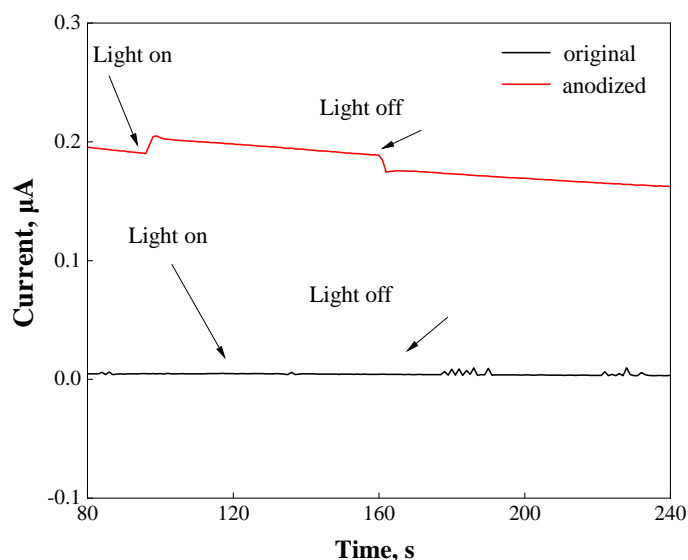


**Figure 6.** The transient photocurrent curve of 304 SS under a thin NaCl electrolyte layer with and without UV irradiation after anodization.

As shown in Figure 6, the natural passive film displayed no significant photoresponsive current, while the anodic pre-passivated film generated a stable photocurrent of about  $0.02 \mu\text{A}$  at the beginning of the light exposure and disappeared without light. The results indicated that the pre-passivated stainless steel developed a thicker passivation film with a strong photo response. Contrary to previous studies [16-18], the weakened pitting resistance of the passive film may be due to the rapid oxygen transport rate under a liquid thin film.

### 3.5. Corrosion mechanism

The corrosion mechanism underlying the thin NaCl electrolyte layer corrosion of 304 SS exposed to UV illumination is shown in Figure 7. The band gap of the passive film in the stainless steel was between 2.2 eV and 3.6 eV. The energy of the UV light at a wavelength of 312 nm was about 3.98 eV, which was sufficient to excite the valence band electrons of the film into the conduction band. Therefore, the generated holes were enriched on the surface of the passive film due to photoexcitation. Therefore, the high  $\text{Cl}^-$  concentration on the surface could be attributed to the electrostatic adsorption of  $\text{Cl}^-$  by the positively charged surface. Chloride ions can reduce the diffusion energy barrier of point defects in solutions [36] and increase the concentration of cation vacancies at the film/solution interface [37]. The adsorbed  $\text{Cl}^-$  destroyed the local passive film to expose the fresh substrate, resulting in pitting.

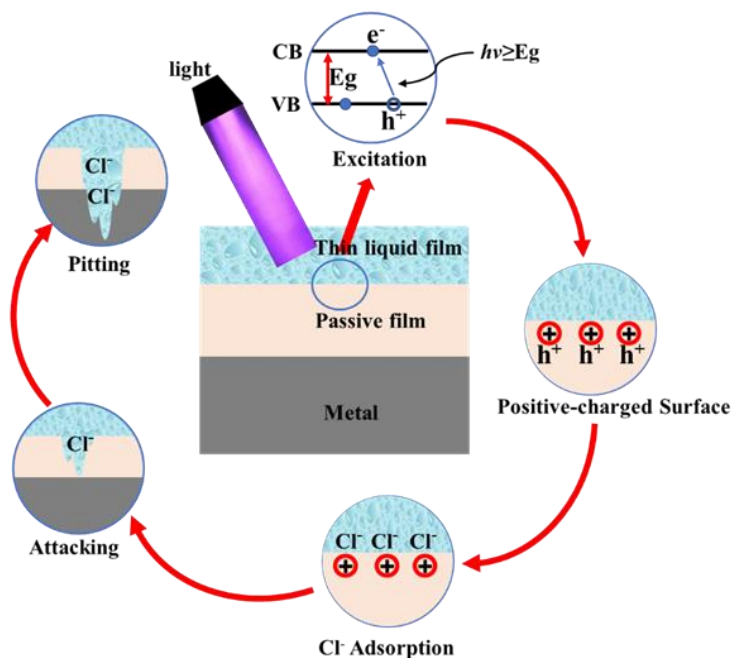


**Figure 7.** Schematic diagram of the rupture of 304 SS passive film with UV irradiation.

The surface potential of the passive film was elevated due to positive charge enrichment. This state further resulted in a higher voltage drop at the passive liquid film/thin film interface, also known as the Helmholtz layer voltage drop. The dissolution rate of the cations in the passive film was positively correlated with the Helmholtz layer voltage drop [38]. In addition, a more significant Helmholtz layer voltage drop yielded higher flat band potential. The Helmholtz layer voltage drop was increased after UV illumination, raising the flat-band potential of the passive film, which was consistent with the M-S test results.

In summary, the causes of the shallow pitting areas on the surface of 304 SS exposed to UV illumination are likely to be extensive. The thin NaCl electrolyte layer is an oxygen-rich environment where light promotes the formation of conductive  $\text{Fe}_3\text{O}_4$  and accelerates the corrosion of the substrate material. Furthermore, UV illumination can induce electrons in the passivated film to participate in the cathodic reaction, allowing hole-electron pair separation. Increasing the  $\text{Cl}^-$  concentration on the positively charged surface accelerates pitting nucleation and development.

#### 4. CONCLUSIONS

The corrosion behavior of 304 SS under a thin electrolyte layer containing  $\text{Cl}^-$  is significantly influenced by UV illumination. The main conclusions obtained in this paper are as follows:

(1) The polarization experiments demonstrate that regardless of whether it is prepassivated or not, pitting corrosion is more likely to occur in UV-irradiated 304 SS under a thin NaCl electrolyte layer, while the light accelerates the corrosion process.

(2) The unexposed specimens display deep pits on the surface, while the light-exposed specimens showed shallow pitting areas. UV illumination of the thin NaCl electrolyte layer may also elicit a

significant photoresponse from the passive film. The cathodic reaction is not hindered, accelerating corrosion due to the oxygen-rich thin electrolyte layer.

(3) UV light can change the corrosion product type. The photoelectric effect caused by the corrosion products with semiconductor properties affects the Cl-induced pitting process of 304 SS after UV illumination.

#### ACKNOWLEDGEMENTS

This investigation was supported by the National Natural Science Foundation of China (No. 20200182).

#### References

1. L.M. Zhang, Z.X. Li, J.X. Hu, A.L. Ma, S. Zhang, E.F. Daniel, A.J. Umoh, H.X. Hu and Y.G. Zheng, *Tribol. Int.*, 155 (2021) 106752.
2. Y. Wang, X. Mu, J.H. Dong, A.J. Umoh and W. Ke, *J. Mater. Sci. Technol.*, 76 (2021) 41.
3. Y.T. Ma, Y. Li and F.H. Wang, *Corros. Sci.*, 51 (2009) 997.
4. A.N. Chen, F.H. Cao, X.N. Liao, W.J. Liu, L.Y. Zheng, J.Q. Zhang and C.N. Cao, *Corros. Sci.*, 66 (2013) 183.
5. C.G. Soares, Y. Garbatov, A. Zayed and G. Wang, *Corros. Sci.*, 51 (2009) 2014.
6. R.W. Lindstrom, J.E. Svensson and L.G. Johansson, *J. Electrochem. Soc.*, 147 (2000) 1751.
7. Y.W. Liu, M.R. Liu, X. Lu and Z.Y. Wang, *Mater. Chem. Phys.*, 277 (2021) 124962.
8. C.L. Li, Y.T. Ma, Y. Li and F.H. Wang, *Corros. Sci.*, 52 (2010) 3677.
9. X.B. Liu and J.P. Liu, *Corros. Sci.*, 115 (2017) 129.
10. L.Y. Guo, S.R. Street, H.B. Mohammed-Ali, M. Ghahari, N. Mi, S. Glanvill, A.D Plessis, C. Reinhard, T. Rayment and A.J. Davenport, *Corros. Sci.*, 150 (2019) 110.
11. I.O. Wallinder and C. Leygraf, *Corros. Sci.*, 43(2001)2379.
12. S. Sabir and A.A. Ibrahim, *Corros. Eng. Sci. Technol.*, 52 (2017) 276.
13. F. Corvo, A.R. Mendoza, M. Autie and N. Betancourt, *Corros. Sci.*, 39 (1997) 815.
14. M.X. Guo, J.R. Tang, C. Peng, X.H. Li, C. Wang, C. Pan and Z.Y. Wang, *Mater. Chem. Phys.*, 276 (2022) 125380.
15. S.H. Mameng, R. Pettersson and C. Leygraf, *Corros. Sci.*, 73(2017)880.
16. D.D. Macdonald and D.F. Heaney, *Corros. Sci.*, 42 (2000) 1779.
17. C.B. Breslin, D.D. Macdonald, E. Sikora and J. Sikora, *Electrochim. Acta*, 42 (1997) 137.
18. S.O. Moussa and M.G. Hocking, *Corros. Sci.*, 43 (2001) 2037.
19. H. Luo, X.G. Li, C.F. Dong, K. Xiao and X.Q. Cheng, *J. Phys. Chem. Solids*, 74 (2013) 691.
20. C.B. Breslin, D.D. Macdonald, J. Sikora and E. Sikora, *Electrochim. Acta*, 42 (1997) 127.
21. S. Fujimoto, T.Y. amada and T. Shibata, *J. Electrochem. Soc.*, 145 (1998) 27.
22. L.Y. Song and Z.Y. Chen, *Corros. Sci.*, 86 (2014) 318.
23. Y.W. Liu, J. Zhang, Y.H. Wei and Z.Y. Wang, *Mater. Chem. Phys.*, 237 (2019) 121855.
24. L.Y. Song, X.M. Ma, Z.Y. Chen and B.R. Hou, *Corros. Sci.*, 87 (2014) 427.
25. L.Y. Song, H. Shi, P. Han, X.H. Ji and F.B. Ma, *J. Ind. Eng. Chem.*, 102 (2021) 206.
26. M.X. Guo, X. Lu, J.R. Tang, C. Pan and Z.Y. Wang, *Int. J. Electrochem. Sci.*, 16 (2021) 210457.
27. Y.L. Cheng, Z. Zhang, F.H. Cao, J.F. Li, J.Q. Zhang, J.M. Wang and C.N. Cao, *Corros. Sci.*, 46 (2004) 1649.
28. H. Sun, X.Q. Wu, E.H. Han and Y.Z. Wei, *Corros. Sci.*, 59 (2012) 334.
29. S. Hastuty, A. Nishikata and T. Tsuru, *Corros. Sci.*, 52 (2010) 2035.
30. M. Stratmann, H. Streckel, K.T. Kim and S. Crockett, *Corros. Sci.* 30 (1990) 715.
31. S.R. Morrison, *Electrochemistry at Semiconductor and Oxidized Metal Electrodes*, (1980) Plenum Press, New York.

32. A.M.P. Simoes, M.G.S. Ferrira, B. Rondot and M.D.C. Belo, *J. Electrochem. Soc.*, 137 (1990) 82.
33. R.M. Fernandez-Domene, E. Blasco-Tamarit, D.M. Garcia-Garcia and J. Garcia Anton, *J. Electrochem. Soc.*, 161 (2014) C25.
34. V. Vignal, C. Valot, R. Oltra, M. Verneau and L. Coudreuse, *Corros. Sci.*, 44 (2002) 1477.
35. Z.H. Dong, W. Shi, G.A. Zhang and X.P. Guo, *Electrochim. Acta*, 56 (2011) 5890.
36. G. Meng, Y. Li, Y. Shao, T. Zhang, Y. Wang and F. Wang, *J. Mater. Sci. Technol.*, 30 (2014) 253.
37. D.I. Seo and J.B. Lee, *Corros. Sci.* 173 (2020) 108789.
38. G. Tranchida, M. Clesi, F. Di Franco, F. Di Quarto and M. Santamaria, *Electrochim. Acta*, 273 (2018) 412.

© 2022 The Authors. Published by ESG ([www.electrochemsci.org](http://www.electrochemsci.org)). This article is an open access article distributed under the terms and conditions of the Creative Commons Attribution license (<http://creativecommons.org/licenses/by/4.0/>).